Smart Agricultural Technology 12 (2025) 101049

Contents lists available at ScienceDirect

Smart Agricultural Technology

journal homepage: www.journals.elsevier.com/smart-agricultural-technology

Detecting copper-based fungicides in vineyards by means of hyperspectral imagery

Ramón Sánchez [a,*], Carlos Rad [b], Carlos Cambra [a], Rocío Barros [c], Álvaro Herrero [a]

[a] Grupo de Inteligencia Computacional Aplicada (GICAP), Departamento de Digitalización, Escuela Politécnica Superior, Universidad de Burgos. Av. Cantabria s/n. 09006 Burgos Spain

[b] Grupo de Investigación en Compostaje (UBUCOMP). Universidad de Burgos. Pl. Misael Bañuelos s/n. 09001, Burgos, Spain

[c] Grupo de Investigación ICCRAM-EST. International Research Center in Critical Raw Materials for Advanced Industrial Technologies (ICCRAM). Universidad de Burgos. Pl. Misael Bañuelos s/n. 09001, Burgos, Spain

ARTICLE INFO

Keywords:
Vineyard
Hyperspectral
Fungicide
Copper
Vine
Agriculture

ABSTRACT

Fungal diseases affecting vineyards are commonly controlled using copper-based fungicides. Inaccurate application of these products usually leads to accumulations of copper in the soil. The use of spectral images in vineyards is a tool that can help in the correct application of fungicides to improve their efficiency and effectiveness. To do that, a solution is required to identify the copper deposited on the vine leaf. To bridge this gap, the present work compares images obtained with a hyperspectral camera (Pika L, Resonon) of vineyard leaves (*Vitis vinifera* L.) cv. Tempranillo treated with two copper-based products, Cuprantol duo (Syngenta, CH) and Cuprocol (Syngenta, CH). Treated leaves with both products and the corresponding blanks made with distilled water were compared. Most of the differences between treatments and products are found in the near-infrared region (700–740 nm), the green region (550 nm) and the region of (620–640 nm). Maximal spectral variations appeared in the range of 711.16–758.27 nm for wet status products, which allowed to differentiate between the areas treated with copper-based products from the blanks without product. We can conclude that using hyperspectral imagery is possible to detect leave areas treated with copper-based fungicides immediately (wet treatment) after application.

1. Introduction

Treating fungal diseases in grapevines with commercial pesticides is a logistical and economic effort that winegrowers face annually worldwide [1]. Copper-based compounds have been widely used for nearly fourteen decades to control phytopathogens [2], and the use of copper is still the most effective way to control these fungal diseases, and particularly, downy mildews [3].

Copper (Cu) is an essential micronutrient taking part in many metabolic reactions such are photosynthetic electron transport, or in the active center of enzymes such as polyphenol oxidase, monoamine oxidase, and other phenolases [4]; however, when in excess, is proved to be harmful to biological systems and can affect human health, considering the possibility of a dietary intake associated with contamination in crops.

Human activities have increased Cu concentration in the environment [5,6]. An incorrect application of copper-based fungicides, by defect or excess, and the drift of the product that is not sprayed towards the vine canopy, ending up in the soil, generates, not only economic losses, but also cumulative contamination of the agricultural soils [7,8] Additionally, incorrect or uncontrolled use of plant protection products can cause an economic damage due to inadequate yields and quality, wildlife damage with undesired effects on non-target species, and environment damage because of a direct pollution [9]

Among copper-based fungicide compounds, some of the most used, and which are important against over 300 diseases on almost 50 food crops, are copper hydroxide ($Cu(OH)_2$), copper oxide (Cu_2O), copper oxychloride ($Cu_2Cl(OH)_3$), and copper sulphate mixtures, commonly referred to as Bordeaux or Burgundy mixtures, which has been intensively used in vineyards since its discover in 1885, not only against downy mildew disease, but also against most of fungal diseases in plants [8]. Consequently, vineyard soils are often more contaminated by Cu than other agricultural soils. This Cu excess accumulates in soil and can impact soil organisms and plants, thereby reducing soil fertility and

* Corresponding author.
E-mail address: ramonsanchezalonso@outlook.es (R. Sánchez).

https://doi.org/10.1016/j.atech.2025.101049
Received 14 March 2025; Received in revised form 23 May 2025; Accepted 24 May 2025
Available online 8 June 2025

productivity [10]. Additionally, leaching and surface runoff export Cu from vineyard soil, which can contaminate aquatic ecosystems and drinking water resources [11]. Some studies report that Cu contamination in vineyard soils induces changes in microbial communities in the surface layers, affecting structural diversity and shifting the resistance of microorganisms to this metal [12,13]. Some authors observed that the high levels of Cu and Zn in the soil were responsible for the reduction of microbial biomass, causing changes in the microbial community with a predominance of acidobacteria phylum in soil with high levels of Cu and Zn [14].

Many worrying cases of pollution regarding copper in vineyard soils were detected at the European Level [11]. Concentrations of Cu in surface horizons of European vineyard soils reach values commonly ranging from 30 up to 290 mg kg^{-1} [11,15]. These values are highly above the warning and critical legislative limits valid in the European Union (EU) which set Cu concentrations in agricultural soils at 50 and 140 mg kg^{-1} [16]. In this way, values ranging between 500 and 600 mg/kg were reported in Spain [17,18], and concentrations around 200–400 mg/kg were found in French soils [19]. Furthermore, in some Croatian vineyards, Cu concentration was found to reach >700 mg kg^{-1} [20].

Fungicide applications in European vineyards range from 4 to 15 sprays per season [21]. Special care should be taken in vineyards with a spatially variable canopy to avoid overdosing in low vigor vines or a lack of coverage or penetration in the most vigorous zones of the plot. Pesticides residues can be detected in the whole grape, including the grape skin [22]. Copper has potential risks to inhibit yeast growth, delay fermentation, and mediate oxidation reactions, which has a huge impact on the nutritional quality and the sensory quality of fresh and aged wine [23].

Precision viticulture (PV) aims to optimize vineyard management, reducing the use of resources, the environmental impact and maximizing the yield and quality of the production. New technologies as unmanned aerial vehicles (UAVs), satellite imaginary, proximal sensors and variable rate machines (VRT) are being developed and used more and more frequently in recent years thanks also to informatics systems able to read, analyze and process a huge amount of data in order to give the winegrowers a decision support system (DSS) for making better decisions at the right place and time [24]. Consequently, there is a present demand for improving spray-based vine treatments in terms of quantifying product depositions: boosting efficiency of deposition, reducing drift and increasing sprayer output.

In this context, the use of multispectral cameras, having few broad- or narrow-bands, usually <20, or hyperspectral, having hundreds of narrow-bands have shown as an effective and non-destructive tool to monitor and analyze in real time the vineyard canopy [25,26]. Furthermore, hyperspectral imagery, could help producers in achieving their efficiency targets, providing real time information [27,28].

Although there are commercial systems that are aimed at determining the correct application percentage of copper products, these are mainly based on indirect determination methods and do not allow real-time monitoring of product application, as is the case with Water Sensitive Papers (WSP). Spectral techniques have proven to be effective in the analysis of nutrients accumulated in grape leaves, using non-destructive methods [29].

Previous studies have demonstrated the effectiveness of combining spectral preprocessing and feature extraction algorithms with machine learning models for the detection of pesticide residues in grapes [30], and also in other cultivars such as tobacco[31] and olive [32], achieving an accuracy superior to 90 %. Up to now, no evidence of previous research using these methods at the vine leaf level has been found. Typically, algorithm deployment requires image datasets as training inputs, which a trained Machine Learning model uses to identify and categorize images. In this work, we present a spectral-based tool capable of identifying regions of interest (RoIs) where the products are located.

The potential savings which can be achieved by the technology proposed in this work and the quality improvement on the soil health, still need to be studied and verified by further field tests. In turn, additional research should be conducted to evaluate whether copper concentration can be successfully reduced while the percentage of treated leaf area increases.

The general objective of this research is to determine the spectral signature of copper when applied in fungicidal products in the form of copper oxide or hydroxide suspensions. Specific objectives are: 1) to develop a procedure to select Cu-treated areas of leaves using hyperspectral images in wet conditions or after drying the product, and 2) to select spectral channels that better reflect the presence of both copper-based products applied at increasing concentrations.

2. Materials and methods

2.1. Rehearsal location

The study was carried out in a vineyard of 16 ha within the Cigales D. O., in North-central Spain (latitude 41° 49′ 17″ N, longitude 4° 35′ 49″ W), 770 m above sea level, in which 134 vine leaves were collected during the months of July and August 2023. The vines (*Vitis vinifera* L.) cv. Tempranillo were grafted on 110-Richter rootstocks, planted at 3.0 × 1.5 m (2222 vines·ha^{-1}), trained in a double cordon Royat system with a vertical positioning of the shoots. The average age of the vineyard was 25 years, and the soil is classified as *Chromic cambisol* according to FAO, with sandy texture.

2.2. Sample preparation

Leaf sampling was carried out during the months of July and August, collecting leaves from different lines of vines exposed to both morning sun (*E*, east exposure) and afternoon sun (*W*, west exposure). In each of these exposures, leaves of different sizes were collected according to their arrangement on the shoot: basal (*S*, basal position, high leaf area), middle position (*M*, medium leaf area), apical position (*S*, tender leaves with small area).

The transport of the samples from the vineyard to the laboratory was carried out under refrigerated conditions, at a temperature of approximately 10 °C. The leaves were treated in the same morning they were collected to avoid dehydration.

2.2.1. Products used

Two antifungal copper based products produced by Syngenta, (Syngenta, CH) were used in this study:

- *ZZ Cuprocol* (70 % w/V copper oxychloride in water)
- *Cuprantol Duo* (140 g/kg (14 % w/w) copper oxychloride, 140 g/kg (14 % w/w) copper hydroxide,)

2.3. Assay with antifungal products

Two assays were made on the sampled leaves concerning this work. A template with 120 deposition holes was created to study spectral differences between both copper-based products at applied at different concentrations and the leaf background. The template was made using a transparent PVC base, featuring deposition holes with a diameter of 0.4 cm using a laser cutting machine. These holes were evenly spaced 1 cm apart. For the deposition of the products, a precision micropipette of 1–10 microliters was used, adding 2 microliters of solution in each deposition location. Two series of the following dilutions were made for each product: 0.20 – 0.33 – 0.40 – 0.66 – 0.80 – 1.33 g L^{-1}, complying with the usual application range of these products [33].

The solutions corresponding to the concentrations of each product were determined using a precision scale and volumetric flasks. Thereafter, the solutions were stored in Falcon-type tubes, and prior to each deposition, these were homogenized using a vortex mixer.

The 120 deposition spots of the template were divided into 6 randomized groups of 20 spots. 18 spots of each group corresponding to the 6 dilutions of each product. Of the remaining 12 spots, 8 of them were used for distilled water blanks and 4 more were used to make black marks for positioning the template in the leaf.

A second trial was conducted on vine leaves, applying the products with a spray, reproducing in the laboratory a similar application to that performed in the vineyard. In this second trial, two hyperspectral photographs were taken for each leaf: one of the leaf without the product and another one of the leaf with the product applied.

2.4. Hyperspectral image acquisition

The hyperspectral camera used in the study is the Pika L model from Resonon (Resonon, USA), that covers the visible and near-infrared with 300 channels in a spectral range of 400 – 1000 nm, a spectral resolution of 2.7 nm and 900 spatial pixels, with a framerate of 64.96. The lens objective is a C-mount with a CMOS sensor type.

The device is attached to a mechanical mobile bench (Resonon, USA) to facilitate scanning, an illumination system was included on the column where the camera was also attached. This system consists of 4 halogens lamps (USHIO MR16, FMW/FG/WS/5300, 12 V 35 W FL36°). The leaves to be photographed on a white PVC tray placed on the mobile bench. The distance between the lens of the camera and the tray where the sample was located was 62 cm (Fig. 1).

2.5. Data pre-processing and statistical analysis

Each pixel in the hyperspectral images has spectral reading values between 0 and 10,000. Following the diagram showed in Fig. 2, from each leaf, all the pixels of the region of interest (product depositions) were manually selected and the spectral readings of the 300 channels (400–1000 nm) were then extracted in two formats: *.txt* and *.xls*, generating a spectral subset, as described in Fig. 2. According to other studies that use a hyperspectral camera to study plant materials, we have found signal noise in the spectra regions between 400 and 450 nm and beyond 900 nm [34], and therefore we have discarded the results included in these channels.

Curated spectral data of the regions corresponding to the product and blank deposition drops, the difference in readings was extracted, channel by channel, to find those channels in which this difference was greater.

A determination was made of the spectral channel that showed the greatest difference in reflectance compared to the blank reading. To achieve this, the average spectrum of all blank samples on the same leaf—created by depositing distilled water—was calculated. The spectral difference between each deposition and the median of the blanks was then computed to identify the channel (mode). The median of the spectral readings of the blanks was calculated to subtract a representative value from each reading of the product depositions. Average values were used for the spectral readings when compared to each other, meanwhile mode values were selected to pick a specific channel. Based on this, a new spectrum was generated, consisting of the difference between the average spectral reading of the product deposition areas and the median spectral reading of the blank areas on each leaf. (Fig. 4).

The sample population varies slightly between different concentrations due to the irregularity of the vine leaves in terms of size and morphology.

An ANOVA analysis of the spectral reading results by product and concentration, for each channel, has been performed to determine the significant differences between treatments. As a complement to this test, the Tukey's test has been carried out to detect treatment groups that present significant differences in terms of products and concentrations.

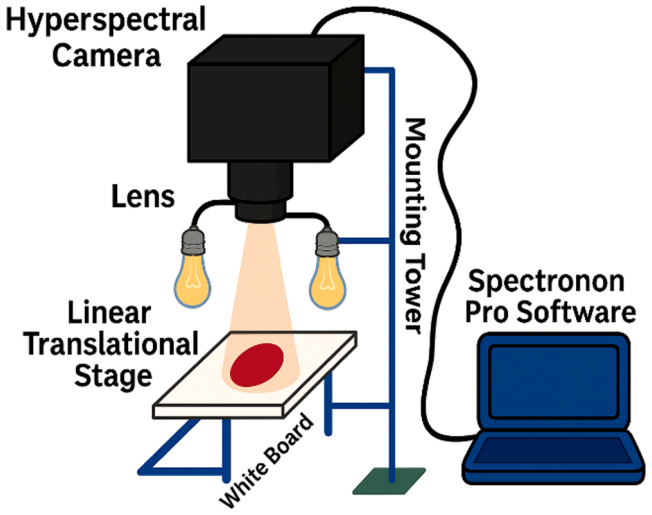

Fig. 1. Benchtop hyperspectral imaging system.

2.6. Computer processing

A computer tool has been developed. Based on hyperspectral images, this tool identifies the contour of the leaf and, by means of a selection of spectral reading ranges, it is able to identify the areas covered by the applied products.

To extract information from the hyperspectral images, each pixel was labelled according to its location in the image: leaf (01), background (00), or product drop (10). This data was saved in a .csv file, from which an image was created, assigning a different colour to each value. Finally, another .csv file was created, containing the percentage of product droplets within the given area of the vine leaf. The process followed is described in Fig. 3.

2.6.1. Leaf outline extraction

To extract the leaf outline, channel 10 (406.68 nm) was selected, as there was a significant difference between the reflectance values of pixels belonging to the image background and those belonging to the leaf itself. This allowed for the creation of a new binarized image in which the pixels belonging to the leaf were separated. The reflectance threshold selected for the pixels forming the interior of the leaf was <2000. To achieve a more uniform binarization, the "remove_small_holes" function (from the "skimage.morphology" library) was applied to fill in any gaps that might appear when obtaining the complete leaf surface.

2.6.2. Droplet and leaf separation

In the process implemented for droplet discrimination, the parameters applied are those derived from the statistics presented in this article. The selected channel is 165 (728.24 nm). If the product to be detected is *Cuprocol*, those pixels that are between 3900 and 4100 (product) and between 4900 and 5200 (water) will be marked as droplets. If the product to be detected is *Cuprantol Duo*, the detection threshold will be pixels with values between 3900 and 4300 nm (product) or between 4900 and 5200 nm (water). This ranges where selected looking at the results presented in the Section 3 of this work. The range corresponding to water (or blank) is included in the algorithm processing so that the detected drops include their entire morphology, since the product accumulates at the edges of the drops and determining coverage would be confusing.

During this double binarization process, a significant amount of noise or false detections was detected when identifying the droplets, because, within the theoretical range for detecting the compounds, there are certain areas on the leaf that have reflectance values within that same range. To eliminate this noise, a technique based on the ORB (Oriented Fast and Rotated Brief) algorithm was developed.

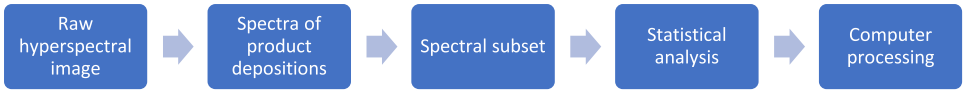

Fig. 2. Preprocessing diagram.

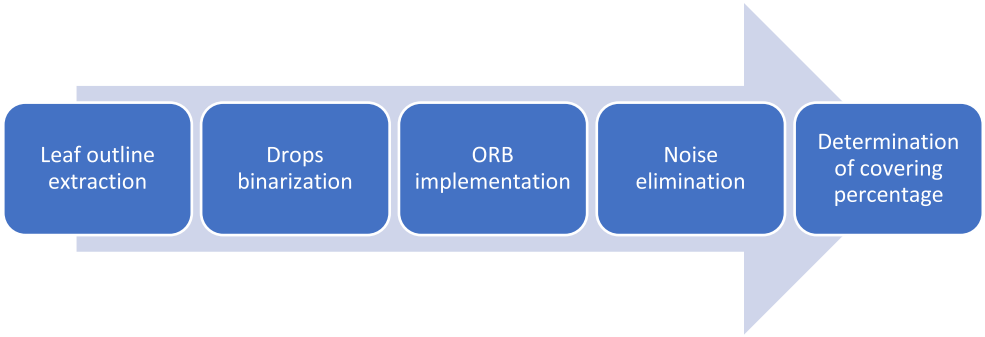

Fig. 3. Computer processing diagram.

2.6.3. Noise removal

As described in the methodology, two images were taken for each leaf, one before applying the product solution and another immediately afterward, both under the same lighting conditions. Pixels that match in both images, spectrally treated with the same parameters, are "subtracted."

First, both images must be aligned to overlap them, using the ORB algorithm for solving problems with rotation and morphological changes, resulting from leaf manipulation when applying the product.

Once both images are binarized and superimposed, which is one of the elements that undergoes the most modifications when comparing the two images, we facilitate the algorithm's work removing the petiole and applying the ORB algorithm. Once the mask with the product droplets defined on the leaf surface is obtained, the percentage of product coverage is calculated by applying the formula (total leaf pixels / pixels marked as product) x 100.

2.6.4. ORB (Oriented fast and rotated BRIEF) algorithm

This algorithm, which comes from the OpenCV library, aims to find relevant points in the image and assign them a descriptor or label that allows, in our case, the images to be superimposed.

Fast is a corner detector, which has been used to detect relevant points on the edges of the leaf. Rotated BRIEF refers to the alignment and transformations necessary for the correct superposition of the images once the key points have been detected and labelled.

3. Results

3.1. Spectral differences between treated leaves and blanks

Attending to the spectra of the differences between spectral readings of the products and the blanks (Fig. 5), the maximum differences are observed in two regions. The region between bands 500–580 nm is where there is a higher positive difference in the spectral data of the copper dropping area with respect to the blank. However, the point that presents a greater absolute difference is found in a more limited region, between bands 726 and 752. Fig. 4 shows two versions of the same photograph, in its real colour and in a single band within the range that

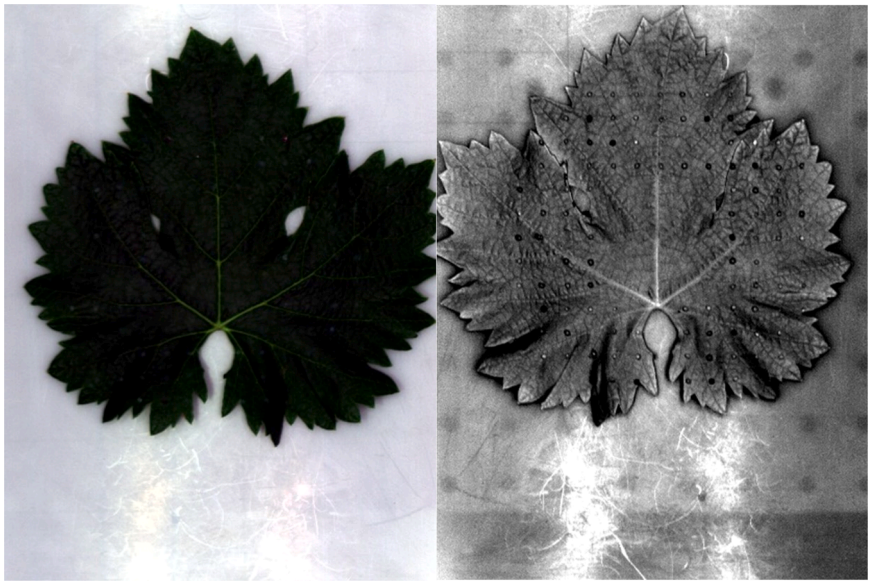

Fig. 4. Difference between the image of a treated leave in its original RGB format (639.1 nm, 549.4 nm, 459.2 nm) (a) and in the band of maximum differences with the blank, 728.20 nm (b).

presents the greatest difference in contrast (728.20 nm), showing the visual result before and after the application of this filter on one of the treated leaves, for the wet treatment. As it is shown in the Fig. 4, the greatest differences between treatments are obtained in the channels where the reading difference is negative.

Fig. 5 displays the difference between the average of the pixels of a product drop and the mean of the blanks of the same leaf. In both graphs there are two points of coincidence in all spectra: an increase in intensity is observed in the green range (550 nm), and in the infrared range (700 nm).

When comparing the spectrum of a drop of product with the spectrum of the blank, we observed that the spectrum of the area treated with product returns higher values in the first half of the spectral curve, from 450 to 700 nm, and lower than the blank as it approaches the near IR region, > 700 nm (Fig. 6).

3.2. Average spectra per product and concentration

Comparing the spectra corresponding to drops of the same product at different concentrations, the shapes of the graphs are similar, but they differ in the intensity of the reflectance. Higher concentrations have higher reflectance in the spectral region between 400 and 700 nm and lower in the next range from 700 to 900 nm (Fig. 7). The differences between the average spectra between 600 nm and 700 nm, as well as the dynamics of the spectra on the near-IR region require further processing.

Fig. 7 shows the spectra of the wet treatments, with higher readings up to the 550 nm zone and lower readings in the infrared region as the concentration of the product in the treatment increases.

A higher spectral average value was observed around the large peak appearing at 550 nm and especially in the near-IR region (750–900 nm). Maximum spectral readings difference with respect to the blanks were determined. The data in Table 1 show the modes of the channels in which the spectral reading has a maximum difference from the blank.

The range of channels displaying the maximum differences between both products and the blank was between 728,24 nm and 745,38 nm (intensity of products lower than blank). The wet treatments of *Cuprocol* showed more discriminating results in the range 728. 24 - 745.38 nm. In the case of *Cuprantol Duo*, the range of channels which showed more difference with the blank readings is even more limited: 736.80 - 745.38 nm.

The ANOVA analysis (see Supplementary Materials) showed that in the wet treatments, the ranges that showed significant differences ($p < 0.05$) are 451.12 nm - 510.29 nm, 601.41 nm – 696.26 nm and 711.16 nm– 899.79 nm. But if we look at the F values, to determine the range where we can find a greater differentiation between the groups, the highest values ($F > 100.00$) are found in the range of channels (nm): 717.56 – 747.53. Moreover, the most pronounced differences are observed from the channel of 723.98 nm with a F-value of 120.82 and $p < 0.001$.

The data have been subjected to the Tukey's test, to find were significant differences appeared with respect to their spectral reading in the different channels. We have analysed the cases individually, by product in wet and dry conditions, and its comparation with the blank's spectra.

In the case of *Cuprantol Duo* (Table 2) in wet images in the range 698.38 nm −726.10 nm, two different groups were obtained. Group 1 included all product concentrations and excluded the blank that was in Group 2. The range of 728.24 nm – 741.10 nm, returned as the most interesting one, differentiating between 3 groups, with Group 3 corresponding only to the concentration of the blank. In the range of 743.24 nm – 899.79 nm we again find a separation into two groups, the first being occupied by the concentrations containing product and the second only represented by the blank.

The statistics for wet treatments showed complexity in the interpretation of the results. Based on Tukey's test, we find the following channel ranges with a statistical separation between both products and the blank: 451.12 nm-516.46 nm, 549.44 nm −557.72 nm, 643.36 nm - 669.68 nm, 696.26 nm – 713.3 nm, 749.68 nm – 899.79 nm. The channel range 715.43 nm – 747.53 nm, has proven to be of special interest, as the three groups present highly significant statistical differences between them.

In the case of *Cuprocol*, the channel range of 698.38 nm-702.64 nm discriminated between two distinct groups. Group 1 included all product concentrations and excluded blank, which was located in Group 2. The spectral differences were very similar for both products in wet, so we have a statistically indicated approximation for the determination of the presence/absence of product in the wet state. In the range of 711.16 nm - 899.79 nm we have the separation of concentrations into 3, 4 and 5 groups, where the last one always corresponds to the concentration of the target. But when we look at the range of channels between 726.10 and 732.52 nm it returns a differentiation between 5 groups of concentration and a clear difference with the blank spectrum, offering the opportunity of discriminating even between product concentrations (Table 3).

The results show the channel of 728.24 nm as a common point for the detection of both copper-based products.

3.3. Validation of the methodology in real sprayed samples

The theoretical method was validated by implementing into the program the ranges for the products in their wet state at the maximum application concentration (1.33 g L^{-1}) (Fig. 8).

In the example shown in Fig. 8, the theoretical ranges for the

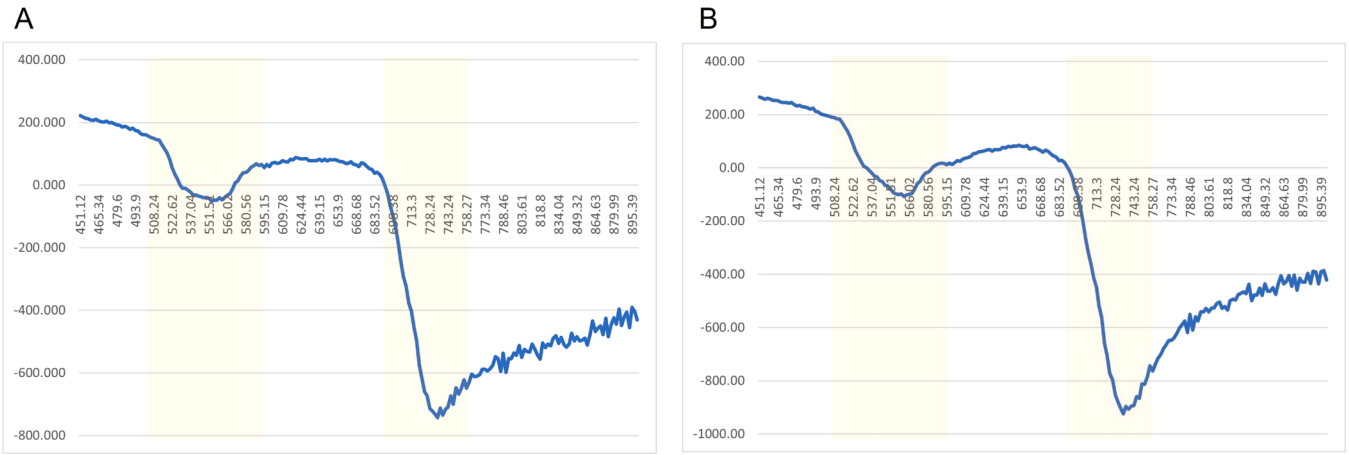

Fig. 5. Spectra of the differential reading graphs between treatments and blanks. A) *Cuprantol Duo* (P1), 1.33 g L^{-1} (C6); B) *Cuprocol* (P2), 1.33 g L^{-1} (C6).

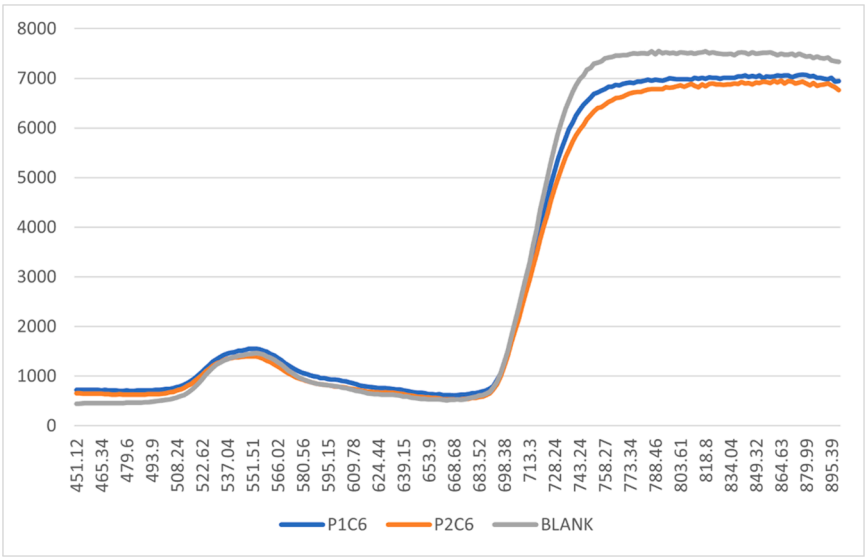

Fig. 6. Spectral differences between the average of the pixels of a drop of wet product on the same leaf (EMwet050723 in the dataset). *Cuprantol Duo* (P1, blue) *Cuprocol* (P2, orange) both at 1.33 g L^{-1} (C6) and the mean of the blanks with water (grey).

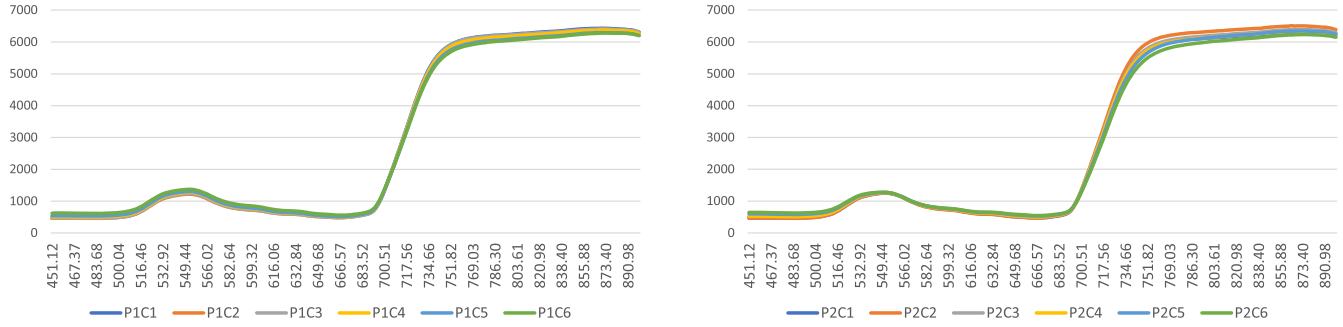

Fig. 7. Average spectra of product 1 and 2 for each concentration (wet treatments). A) *Cuprantol Duo* (P1) and B) *Cuprocol* (P2) at different concentrations: C1: 0.20; C2: 0.33; C3:0.40; C4: 0,66; C5:0,80; C6: 1,33 g L^{-1}.

Table 1
Mode of the wavelengths (nm) with the maximum positive and negative spectral difference against the blanks. Concentration: C1: 0.20; C2: 0.33; C3: 0.40; C4: 0.66; C5:0.80; C6: 1.33 g L^{-1}.

	Cuprocol	*Cuprantol Duo*
C1	728.24	745.38
C2	728.24	734.66
C3	730.38	743.24
C4	745.38	738.96
C5	734.66	743.24
C6	736.80	736.80

maximum concentration of *Cuprocol* (1.33 g L^{-1}) have been implemented in practice. The leaf treated with conventional spray, simulating the actual application conditions in the vineyard, is identified in the dataset as « *EM 1 300,823* ».

To obtain this first image, the 728.24 nm channel was selected, and pixels within the range of the highest concentration (4092.55) were displayed. We selected results that showed all pixels within the leaf with readings between 3800 and 4100 nm.

To identify pixels corresponding to noise readings (i.e. areas of the leaf within this range), a hyperspectral image was taken from the leaf prior to product deposition (Fig. 8.b) and after the spray treatment (Fig. 8.a). Those matching pixels were then discarded (Fig. 8.c).

The results show an approach to determining the effectiveness of a product's application in real time, accurately, and in a manner

Table 2
Tukey's test of *Cuprantol Duo* in wet conditions for reflectance in the channel 728.24 nm. Concentration: C1: 0.20; C2: 0.33; C3: 0.40; C4: 0.66; C5:0.80; C6: 1.33 g L^{-1} and the blank.

728.24 nm				
Tukey HSD[a,b]				
concentration	N	Subset for alpha = 0.05		
		1	2	3
6	61	4360.76		
5	58	4411.03	4411.03	
4	65	4492.37	4492.37	
2	58	4505.46	4505.46	
3	58	4527.99	4527.99	
1	54		4558.32	
Blank	93			5019.07
Sig.		0.16	0.29	1.00

Means for groups in homogeneous subsets are displayed.
[a] Uses Harmonic Mean Sample Size = 62.071.
[b] The group sizes are unequal. The harmonic mean of the group sizes is used. Type I error levels are not guaranteed.

Table 3
Tukey's test of *Cuprocol* in wet conditions for reflectance in the channel 728.24 nm. Concentration: C1: 0.20; C2: 0.33; C3: 0.40; C4: 0.66; C5:0.80; C6: 1.33 g L^{-1} and the blank.

728.24						
Tukey HSD[a,b]						
concentration	N	Subset for alpha = 0.05				
		1	2	3	4	5
6	69	4092.55				
5	63	4244.43	4244.43			
4	65		4366.72	4366.72		
3	60		4408.06	4408.06	4408.06	
1	63			4438.76	4438.76	
2	65				4558.85	
Blank	93					5019.07
Sig.		0.17	0.11	0.91	0.18	1.00

Means for groups in homogeneous subsets are displayed.
[a] Uses Harmonic Mean Sample Size = 67.032.
[b] The group sizes are unequal. The harmonic mean of the group sizes is used. Type I error levels are not guaranteed.

adaptable to the selected product and its concentration based on the spectral reading.

4. Discussion

In the context of the determination of the efficiency of copper-based pesticides, this study explored the efficacy of using hyperspectral imaging processing to determine the product application at increasing concentrations. The resulting spectra showed different behaviour when they are determined for each of the tested products, *Cuprantol Duo* and *Cuprocol*, as well as when we look at the applied concentrations.

Most of the differences between treatments and products are found in the near-infrared region (700–740 nm), the green region (550 nm) and the region of (620–640 nm). These results are consistent with other studies carried out in vineyards, that describe this ranges as the most probable to show mean differences on leaves when submitted to hyperspectral analysis [35]. According to other authors the peak showed at 550 nm corresponds to the anthocyanin reflection of the red light, that occurs in that region [36]. The region of 700–740 nm is the one that has shown the greatest capacity for differentiation the products from the blank treatments. This range of channels, on the near-IR spectrum, is reported to be especially sensitive to plant stress [37,38]

In our study, the spectral channels between 723.98 nm and 758.27 nm have shown the greatest differences for both theoretical and practical discrimination, in terms of imaging processing for the copper-based products, at least when they are applied on this variety of vine leaves (cv. Tempranillo).

When the data was submitted to Tukey test, the channel 728.24 nm appeared as a meeting point for the cases studied, since the greatest discriminations between products, products and blanks and concentrations were obtained around this specific channel in the wet treatments. This selected channel could vary depending on the compound used even if the rest of conditions were similar. These results differ with studies made on the detection of pesticides on grapes, that select the channels ranges 470–530, 650–690 and 760–900 nm as the ones that showed more effectiveness [30]. Other study, on spinach leaves that were treated with different concentrations of dimethoate, selected the hyperspectral region of 900 to 1700 nm to identify the residue, with an accuracy of 99.70 % [39].

The method and the results presented in this work showed that besides the complexity of the interpretation of spectral data dynamics when treating copper-based products applied to vine leaves, there are a big potential of the hyperspectral imaging to determine the correct application of copper-based pesticides and also other non-copper products (data not presented).

Due to the variable nature of spectral imaging, solutions that have been proposed for the application of this specific copper compounds on leaves of cv. Tempranillo, cannot be generalized to another cultivar without a careful testing. In the current moment of this investigation there is a limited spectral data availability to make further conclusions. Despite the developed solution's limitations, its value to vineyards production is substantial as it provides a proof of concept for developing new tools to determine the percentage of total leaf area covered by plant protection products (PPPs), thus facilitating the optimization of their application, improve the efficiency, reduce environmental impact and increase economic benefits. Further research is required on how different PPPs influence the reflectance. The results achieved in terms of spectra analysis, suggests this method could be useful in agricultural tasks.

Other studies have demonstrated the possibility of using non-image-based hyperspectral methods for evaluating foliar fungicide efficacy, such as leaf clip or hyperspectral spectroradiometer [40]. However, these methods provide partial, slower and less precise information than techniques involving hyperspectral image processing.

The findings of this study are of particular interest in terms of the fact that computer methods based on hyperspectral technology prove to be more accurate, efficient and economical than traditional methods,

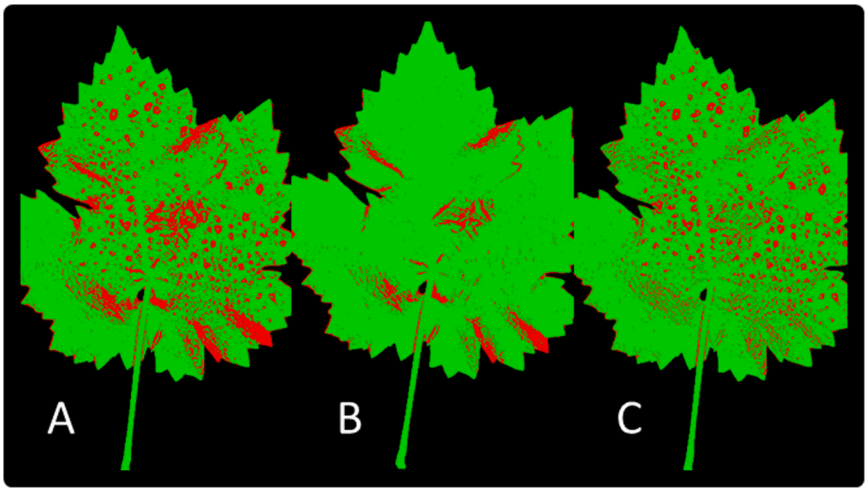

Fig. 8. a) Treated leave with *Cuprocol* 1.33 g L^{-1} in the spectral range 3300–4100 nm; b) non-treated leaf in the same selected range; c) difference between spectral readings.

which are much more rudimentary, complex in their practical implementation, and with longer-lasting results.

The study has certainly limitations, as it was done on a single grape variety and using selected products. Future research should compare the results with other crops and products, drawing new conclusions on this innovative application. As a complementary quantitative copper measurement and carry out a pixel-level validation we propose a methodology, implementing the use of microscopic image of the droplets that must be captured using a SEM-EDS microscope. These images would show the pixel-by-pixel distribution of copper. Overlaying SEM-EDS and hyperspectral images of the same product droplet would allow further validation of the method.

5. Conclusions

The findings in our study demonstrate that spectral analysis can be a useful tool to differentiate the areas of the leaf that are treated with copper-based fungicides at different concentrations and in both wet and dry conditions. This aspect is a necessary condition for an image-based system able to calculate the percentage of successful covered canopy at the time of application and thus, be able to correct the gaps of lacking product. However, it requires greater proficiency in the use of specific algorithms. With the use of the computational method proposed in this work, it will be possible to replace direct observation or the using of different tools that have proven to be less precise such as WSP and propose a viable and real-time solution tools for proximal and remote agriculture applications.

Funding

This publication and the related dataset are part of the DIG4VITIS project (reference TED2021–131551B-I00) funded by MCIN/AEI/10.13039/501100011033 and the European Union ("NextGenerationEU*/PRTR.).

Ethics statement

Not applicable: This manuscript does not include human or animal research.

Safety statement

The authors state that during the application and manipulation of the products in the laboratory all safety protocols have been followed: gloves, masks, glasses and body protection had been implemented. None of the applications have been made in the field for this study. The product waste management proceed has followed the University of Burgos protocol (*Manual de gestión de residuos peligrosos*).

CRediT authorship contribution statement

Ramón Sánchez: Writing – review & editing, Methodology, Investigation, Formal analysis. **Carlos Rad:** Writing – review & editing, Supervision, Methodology, Conceptualization. **Carlos Cambra:** Writing – review & editing, Supervision, Methodology, Conceptualization. **Rocío Barros:** Writing – review & editing, Conceptualization. **Álvaro Herrero:** Writing – review & editing, Supervision, Methodology, Conceptualization.

Declaration of competing interest

The authors declare that they have no known competing financial interests or personal relationships that could have appeared to influence the work reported in this paper.

Acknowledgements

The authors would also like to acknowledge Valdelosfrailes cellar, belonging to winery MATARROMERA S.L. and Syngenta for providing leaves and pesticide samples, respectively.

Supplementary materials

Supplementary material associated with this article can be found, in the online version, at doi:10.1016/j.atech.2025.101049.

Data availability

https://riubu.ubu.es/handle/10259/8759.

References

[1] M.C. Fontaine, et al., Europe as a bridgehead in the worldwide invasion history of grapevine downy mildew, plasmopara viticola, Curr. Biol. 31 (10) (May 2021), https://doi.org/10.1016/j.cub.2021.03.009, 2155-2166.e4.
[2] Y. Yu, H. Liu, H. Xia, Z. Chu, Double- or triple-tiered protection: prospects for the sustainable application of copper-based antimicrobial compounds for another fourteen decades, Int. J. Mol. Sci. 24 (13) (Jun. 2023) 10893, https://doi.org/10.3390/ijms241310893.
[3] K. Koledenkova, Q. Esmaeel, C. Jacquard, J. Nowak, C. Clément, E.Ait Barka, Plasmopara viticola the causal agent of downy mildew of grapevine: from its taxonomy to disease management, Front. Media S.A (May 11, 2022), https://doi.org/10.3389/fmicb.2022.889472.
[4] F. Errichiello, et al., Copper (II) level in musts affects acetaldehyde concentration, phenolic composition, and chromatic characteristics of red and white wines, Molecules. 29 (12) (Jun. 2024), https://doi.org/10.3390/molecules29122907.
[5] P.K. Rai, S.S. Lee, M. Zhang, Y.F. Tsang, K.H. Kim, Heavy Metals In Food Crops: Health Risks, Fate, Mechanisms, And Management, Elsevier Ltd, Apr. 01, 2019, https://doi.org/10.1016/j.envint.2019.01.067.
[6] V. Kumar, et al., Copper Bioavailability, Uptake, Toxicity And Tolerance In Plants: A Comprehensive Review, Elsevier Ltd, Jan. 01, 2021, https://doi.org/10.1016/j.chemosphere.2020.127810.
[7] A. De Bernardi, E. Marini, C. Casucci, L. Tiano, F. Marcheggiani, C. Vischetti, Copper monitoring in vineyard soils of Central Italy subjected to three antifungal treatments, and effects of sub-lethal Copper doses on the earthworm eisenia fetida, Toxics 10 (6) (Jun. 2022), https://doi.org/10.3390/toxics10060310.
[8] M. Komárek, E. Čadková, V. Chrastný, F. Bordas, J.C. Bollinger, Contamination of Vineyard Soils With fungicides: A review of Environmental and Toxicological Aspects, Elsevier Ltd, 2010, https://doi.org/10.1016/j.envint.2009.10.005.
[9] P.J. Zarco-Tejada, et al., Assessing vineyard condition with hyperspectral indices: leaf and canopy reflectance simulation in a row-structured discontinuous canopy, Remote Sens. Env. 99 (3) (Nov. 2005) 271–287, https://doi.org/10.1016/j.rse.2005.09.002.
[10] M. Hendgen, et al., Effects of different management regimes on microbial biodiversity in vineyard soils, Sci. Rep. 8 (1) (Dec. 2018), https://doi.org/10.1038/s41598-018-27743-0.
[11] B. Droz, et al., Copper content and export in European vineyard soils influenced by climate and soil properties, Env. Sci. Technol. 55 (11) (Jun. 2021) 7327–7334, https://doi.org/10.1021/acs.est.0c02093.
[12] E. Dell'Amico, M. Mazzocchi, L. Cavalca, L. Allievi, V. Andreoni, Assessment of bacterial community structure in a long-term copper-polluted ex-vineyard soil, Microbiol. Res. 163 (6) (2008) 671–683, https://doi.org/10.1016/j.micres.2006.09.003.
[13] D.P.H. Lejon, N. Pascault, L. Ranjard, Differential copper impact on density, diversity and resistance of adapted culturable bacterial populations according to soil organic status, Eur. J. Soil. Biol. 46 (2) (Mar. 2010) 168–174, https://doi.org/10.1016/j.ejsobi.2009.12.002.
[14] J. Song, et al., Effects of Cd, Cu, Zn and their combined action on microbial biomass and bacterial community structure, Environ. Pollut. 243 (Dec. 2018) 510–518, https://doi.org/10.1016/j.envpol.2018.09.011.
[15] L.A. Brun, J. Maillet, J. Richarte, P. Herrmann, and J.C. Remy, "Relationships between extractable copper, soil properties and copper uptake by wild plants in vineyard soils".
[16] Y. Weixin, et al., DIR 86-278 pdf_tcm30-73031, Foods. 11 (1609) (2022).
[17] J.C. Nóvoa-Muñoz, J.M.G. Queijeiro, D. Blanco-Ward, C. Álvarez-Olleros, A. Martínez-Cortizas, E. García-Rodeja, Total copper content and its distribution in acid vineyards soils developed from granitic rocks, Sci. Total. Environ. 378 (1–2) (May 2007) 23–27, https://doi.org/10.1016/j.scitotenv.2007.01.027.
[18] M. Pateiro-Moure, C. Pérez-Novo, M. Arias-Estévez, E. López-Periago, E. Martínez-Carballo, J. Simal-Gándara, Influence of copper on the adsorption and desorption of paraquat, diquat, and difenzoquat in vineyard acid soils, J. Agric. Food Chem. 55 (15) (Jul. 2007) 6219–6226, https://doi.org/10.1021/jf071122e.
[19] A.R. Jacobson, S. Dousset, N. Guichard, P. Baveye, F. Andreux, Diuron mobility through vineyard soils contaminated with copper, Environ. Pollut. 138 (2) (Nov. 2005) 250–259, https://doi.org/10.1016/j.envpol.2005.04.004.

[20] M. Romiae, D. Romiae, and D. Dolanjski, "Heavy metals accumulation in topsoils from the wine-growing regions part 1. Factors which control retention," 2004.
[21] I. Pertot, et al., A critical review of plant protection tools for reducing pesticide use on grapevine and new perspectives for the implementation of IPM in viticulture, Crop. Prot. 97 (Jul. 2017) 70–84, https://doi.org/10.1016/j.cropro.2016.11.025.
[22] M.J. Teixeira, A. Aguiar, C.M.M. Afonso, A. Alves, M.M.S.M. Bastos, Comparison of pesticides levels in grape skin and in the whole grape by a new liquid chromatographic multiresidue methodology, Anal. Chim. Acta (Jun. 2004) 333–340, https://doi.org/10.1016/j.aca.2003.11.077.
[23] J. Wang, et al., Copper in Grape and Wine industry: Source, presence, Impacts On Production and Human health, and Removal Methods, John Wiley and Sons Inc, May 01, 2023, https://doi.org/10.1111/1541-4337.13130.
[24] M. Ammoniaci, S.-P. Kartsiotis, R. Perria, P. Storchi, and F. Marinello, "State of the art of monitoring technologies and data processing for precision viticulture," 2021, doi: 10.3390/agriculture.
[25] R. Tosin, et al., Assessing predawn leaf water potential based on hyperspectral data and pigment's concentration of Vitis vinifera L. in the Douro Wine Region, Sci. Hortic. 278 (Feb. 2021), https://doi.org/10.1016/j.scienta.2020.109860.
[26] S.F. Di Gennaro, P. Toscano, M. Gatti, S. Poni, A. Berton, A. Matese, Spectral comparison of UAV-based hyper and multispectral cameras for precision viticulture, Remote Sens. 14 (3) (Feb. 2022), https://doi.org/10.3390/rs14030449.
[27] S. Gutiérrez, J. Tardaguila, J. Fernández-Novales, M.P. Diago, On-the-go hyperspectral imaging for the in-field estimation of grape berry soluble solids and anthocyanin concentration, Aust. J. Grape Wine Res. 25 (1) (Jan. 2019) 127–133, https://doi.org/10.1111/ajgw.12376.
[28] J. Abdulridha, Y. Ampatzidis, P. Roberts, S.C. Kakarla, Detecting powdery mildew disease in squash at different stages using UAV-based hyperspectral imaging and artificial intelligence, Biosyst. Eng. 197 (Sep. 2020) 135–148, https://doi.org/10.1016/j.biosystemseng.2020.07.001.
[29] J.I. Manzano, M. Rodríguez-Febereiro, M. Fandiño, M. Vilanova, J.J. Cancela, Spectroscopic analysis (UV-VIS-NIR) for predictive modeling of macro and micronutrients in grapevine leaves, Smart Agric. Technol. 10 (Mar. 2025), https://doi.org/10.1016/j.atech.2025.100812.
[30] W. Ye, et al., Detection of pesticide residue level in grape using hyperspectral imaging with machine learning, Foods 11 (11) (Jun. 2022), https://doi.org/10.3390/foods11111609.
[31] M. Liang, Z. Wang, Y. Lin, C. Li, L. Zhang, Y. Liu, Study on detection of pesticide residues in tobacco based on hyperspectral imaging technology, Front. Plant Sci. 15 (Sep. 2024), https://doi.org/10.3389/fpls.2024.1459886.
[32] D.M. Martínez Gila, D. Bonillo Martínez, S. Satorres Martínez, P.Cano Marchal, J. Gámez García, Non-invasive detection of pesticide residues in freshly harvested olives using hyperspectral imaging technology, Smart Agric. Technol. 9 (Dec. 2024), https://doi.org/10.1016/j.atech.2024.100644.
[33] E. Gil, J. Llorens, A. Landers, J. Llop, L. Giralt, Field validation of dosaviña, a decision support system to determine the optimal volume rate for pesticide application in vineyards, Eur. J. Agron. 35 (1) (Jun. 2011) 33–46, https://doi.org/10.1016/j.eja.2011.03.005.
[34] M. Kanning, I. Kühling, D. Trautz, T. Jarmer, High-resolution UAV-based hyperspectral imagery for LAI and chlorophyll estimations from wheat for yield prediction, Remote Sens. 10 (12) (Dec. 2018), https://doi.org/10.3390/rs10122000.
[35] Y.Mickey Wang, B. Ostendorf, V. Pagay, Evaluating the potential of high-resolution hyperspectral UAV imagery for grapevine viral disease detection in Australian vineyards, Int. J. Appl. Earth. Obs. Geoinf. 130 (Jun. 2024), https://doi.org/10.1016/j.jag.2024.103876.
[36] L.R. Gutha, L.F. Casassa, J.F. Harbertson, and R.A. Naidu, "Modulation of flavonoid biosynthetic pathway genes and anthocyanins due to virus infection in grapevine (Vitis vinifera L.) leaves," 2010. [Online]. Available: http://www.biomedcentral.com/1471-2229/10/187.
[37] D.N.H. Horler, M. Dockray, J. Barber, The red edge of plant leaf reflectance, Int. J. Remote Sens. 4 (2) (1983) 273–288, https://doi.org/10.1080/01431168308948546.
[38] K.L. Smith, M.D. Steven, J.J. Colls, Use of hyperspectral derivative ratios in the red-edge region to identify plant stress responses to gas leaks, Remote Sens Env. 92 (2) (Aug. 2004) 207–217, https://doi.org/10.1016/j.rse.2004.06.002.
[39] R.E.N. Zhan-qi, R.A.O. Zhen-hong, J.I. Hai-yan, Identification of Different Concentrations Pesticide Residues of Dimethoate on Spinach Leaves By Hyperspectral Image Technology, Elsevier B.V., Jan. 2018, pp. 758–763, https://doi.org/10.1016/j.ifacol.2018.08.104.
[40] N. Gambhir, et al., Non-destructive monitoring of foliar fungicide efficacy with hyperspectral sensing in grapevine, Phytopathology 114 (2) (Feb. 2024) 464–473, https://doi.org/10.1094/PHYTO-02-23-0061-R.